ARMA 20–1103

Effect of Grain Geometry and Grain Arrangement on the Behavior of Bonded Block Models for Prediction of Brittle Rock Damage

Contreras Inga, C.E., Walton, G., and Holley, E.
Colorado School of Mines, Golden, Colorado, United States

This paper was prepared for presentation at the 54th US Rock Mechanics/Geomechanics Symposium held in Golden, Colorado, USA, 28 June-1 July 2020. This paper was selected for presentation at the symposium by an ARMA Technical Program Committee based on a technical and critical review of the paper by a minimum of two technical reviewers. The material, as presented, does not necessarily reflect any position of ARMA, its officers, or members. Electronic reproduction, distribution, or storage of any part of this paper for commercial purposes without the written consent of ARMA is prohibited. Permission to reproduce in print is restricted to an abstract of not more than 200 words; illustrations may not be copied. The abstract must contain conspicuous acknowledgement of where and by whom the paper was presented.

ABSTRACT: In laboratory-scale numerical simulations of rock damage, the grain structure is commonly approximated through an assembly of bonded Voronoi blocks, and a set of properties that represents the micro-mechanical properties of the grains and grain contacts is calibrated to numerically replicate the macro-mechanical behavior of the rock. Such assemblies provide reasonable approximations of actual grain structures. However, the random nature of Voronoi assemblies increases the uncertainty of the contact micro-properties obtained from the calibration process, potentially leading to incorrect estimations of the rock strength. This study evaluates how different representations of the grain structure, in terms of grain geometry and grain arrangement influence predictions of brittle rock mechanical behavior. Different 2D Bonded Block Models of granite specimens were generated and used as a basis for Uniaxial Compressive Strength test simulations. The quality of agreement between the strength of actual granite specimens and the strength predicted using Bonded Block Models was tested through a comparative analysis. The modeling results show a notable influence of grain shape and grain arrangement. The results also prove that it is possible to predict the strength of rock with reasonable accuracy (within 13% of variability) using reasonably simplified representations of the grain structure in Voronoi models and previously published micro-properties.

1. INTRODUCTION

It is well known that the grain structure of a rock controls the micro-mechanical behavior of the grains, and consequently, the macro-mechanical behavior of a rock (Gao et al., 2016; Wang and Cai, 2018). The mechanical behavior and strength of rocks are usually characterized using laboratory tests such as uniaxial compression, triaxial compression, and tensile tests. Laboratory studies show how individual rock specimens can exhibit different fracturing behavior as well as different strength even when they are the same rock type (Liu et al., 2018). The reason for such differences is the heterogeneous nature of rocks. At the grain-scale, rocks are composed of diverse minerals (i.e., mineral grains) in different shapes and sizes and are also affected by different defects (e.g., micro-cracks). That micro-structural heterogeneity governs a complex micro-mechanical behavior that generates localized stress concentrations within a rock specimen and ultimately results in fracture development (Gao et al., 2016; Wang and Cai, 2018).

As defined previously, the sources of heterogeneity of intact rock are: (i) grain-geometry heterogeneity associated with the variability of size and shape of the grain structure; (ii) grain-scale deformability heterogeneity related to the contrasts in density and elastic properties of different mineral phases; and (iii) grain-grain contact heterogeneity connected to the variation of contact distribution and stiffness anisotropy (Lan et al., 2010; Farahmand and Diederichs, 2015; Wang and Cai, 2018).

In recent decades, thanks to significant developments in computer power, numerical modeling has become a useful tool to quantitatively investigate fracturing processes in brittle rock (Jing, 2003). Continuum, discontinuum, and hybrid continuum-discontinuum methods can be used to conduct brittle rock failure modeling (Potyondy and Cundall, 2004). The continuum approach represents rock damage with a constitutive relation and associated failure criterion in the form of elastic-plastic, elastic-brittle, or strain-softening models. One disadvantage of the continuum approach is its inability to explicitly represent progressive failure in rocks (Wang and Cai, 2018).

In contrast, the discontinuum and hybrid continuum-discontinuum approaches depict rocks as assemblies of discrete particles or blocks. Such approaches model fracturing processes in an explicit manner without the need for pre-defined constitutive models (Wang and Cai, 2018). These two last methods are widely used to model brittle rock mechanical behavior under different loading conditions, such as unconfined and confined compression, or direct and indirect tension. The Discrete

Element Method (DEM) is the most commonly applied discontinuum approach, whereas the Finite Discrete Element Method (FDEM) is the most commonly applied hybrid approach.

In numerical modeling, different approaches have been developed to address intact rock heterogeneity from the point of view of grain geometry, and specifically grain shape. Among DEM models, Bonded Particle Models (BPM) and Bonded Bock Models (BBM) are the most common representations of the grain structure. BPMs represent the rock using disks in two-dimensional (2D) models, and spheres in three-dimensional (3D) models (Potyondy and Cundall, 2004). BBMs depict grain structures using triangular or polygonal shapes in 2D, and tetrahedral or polyhedral shapes in 3D (Jing and Hudson, 2002; Ghazvinian et al., 2014; Lisjak and Grasselli, 2014). The polygonal and polyhedral grain structures, compared with other grain shape assemblies, have achieved the most realistic depiction of the rock's microstructure from the grain-geometry perspective (Wang and Cai, 2018). Voronoi tessellation is commonly used to generate polygonal and polyhedral grain structures for BBMs and has been widely applied (Ghazvinian et al., 2014; Farahmand and Diederichs, 2015; Quey and Renversade, 2018).

Generally speaking, the macroscopic mechanical response to loading of a BBM depends on three different factors: numerical model physics, micro-properties, and grain structure attributes. The numerical model physics include the various fundamental properties of the solution approach (e.g., explicit time-stepping) as well as any relevant boundary conditions. The micro-properties are highly relevant in numerical simulations since they represent both the grain and grain-to-grain contact elastic and strength properties and define the way grains interact with each other within a rock structure. Finally, the grain structure attributes include all the geometric features that define the geometry of grains within a rock, and consequently, the local loading conditions. "Conventional" Voronoi models only consider basic features of the grain structure to represent the grain structure, whereas more complex BBMs can include even small-scale features that add complexity and realism to the models. Simplifications to the grain structure in conventional Voronoi models have consequences for the micro-properties that are derived from the calibration of BBMs to macroscopic laboratory test data. For example, individual grain boundaries, in reality, can have a great deal of small-scale roughness and interlocking but are typically represented as straight lines in BBMs. Accordingly, a conventional BBM calibrated to rock with significant grain-grain contact roughness at scales smaller than what can be represented using a Voronoi geometry might end up with a higher friction angle than the true mineral-mineral contact friction. The further a Voronoi representation in a BBM deviates from the true grain structure, the more the microparameters derived from matching model attributes to laboratory test data represent pure calibration parameters as opposed to fundamental material properties. The degree to which BBM micro-properties approximate fundamental material properties and the corresponding degree to which the Voronoi grain structure approximates true grain structures has not been studied in the literature.

The objective of the present study is to assess the influence of the representation of grain geometry and grain structure arrangement on the macro-mechanical response for prediction of brittle rock mechanical behavior. This study uses 2D Voronoi BBMs that approximate the grain structure of Wausau granite in combination with a set of calibrated micro-properties selected from the literature to assess the impact of different geometric aspects of the grain structure (i.e., grain size, grain shape, and grain arrangement) on UCS test simulations. Comparative analyses were performed to identify the most critical aspects of grain structure representation for assessment of rock macro-properties and rock strength.

2. WAUSAU GRANITE

To predict brittle rock mechanical behavior, this study uses 2D BBMs in combination with a set of micro-properties selected from the literature. The Wausau granite was selected as the subject of this study because its mineral composition and average grain size are similar to Lac du Bonnet granite (Lan et al., 2010; Chen and Konietzky, 2014; Farahmand and Diederichs, 2015). This study uses published values for Lac du Bonnet granite micro-properties in the numerical simulations to test whether it is possible to accurately predict the strength of a rock using previously calibrated micro-properties of another rock with similar characteristics.

The Wausau granite is a dark red alkali-feldspar granite from Marathon County, Wisconsin (LaBerge and Myers, 1983; Sims et al., 1993). For this study, specimens of Wausau granite were obtained from a quarry. The specimens of Wausau granite were characterized through hand-sample petrography, thin-section microscopy, and Scanning Electron Microscopy (SEM)-based automated mineralogy. Three standard thin sections were prepared from a single core specimen for the microscopy analyses. The automated mineralogy analyses were conducted on a TESCAN-VEGA-3 Integrated Mineral Analyzer (TIMA) model LMU VP-SEM. Spectral data were acquired using four energy dispersive X-ray (EDX) spectrometers with a beam stepping interval (i.e., spacing between acquisition points) of 15 μm, an acceleration voltage of 24 keV, and a beam intensity of 14.

According to the SEM-based automated mineralogy analyses, the average mineral composition of the Wausau granite is 24% K-feldspar, 41% plagioclase (albite), 32% quartz, and 3% mafic and accessory minerals (mainly biotite). The apparent grain sizes range from 0.1 mm to 7.0 mm, with a mean grain size of 2.0 mm. Figure 1 shows a photograph of a disk-shaped specimen and a microphotograph of a thin section of Wausau granite.

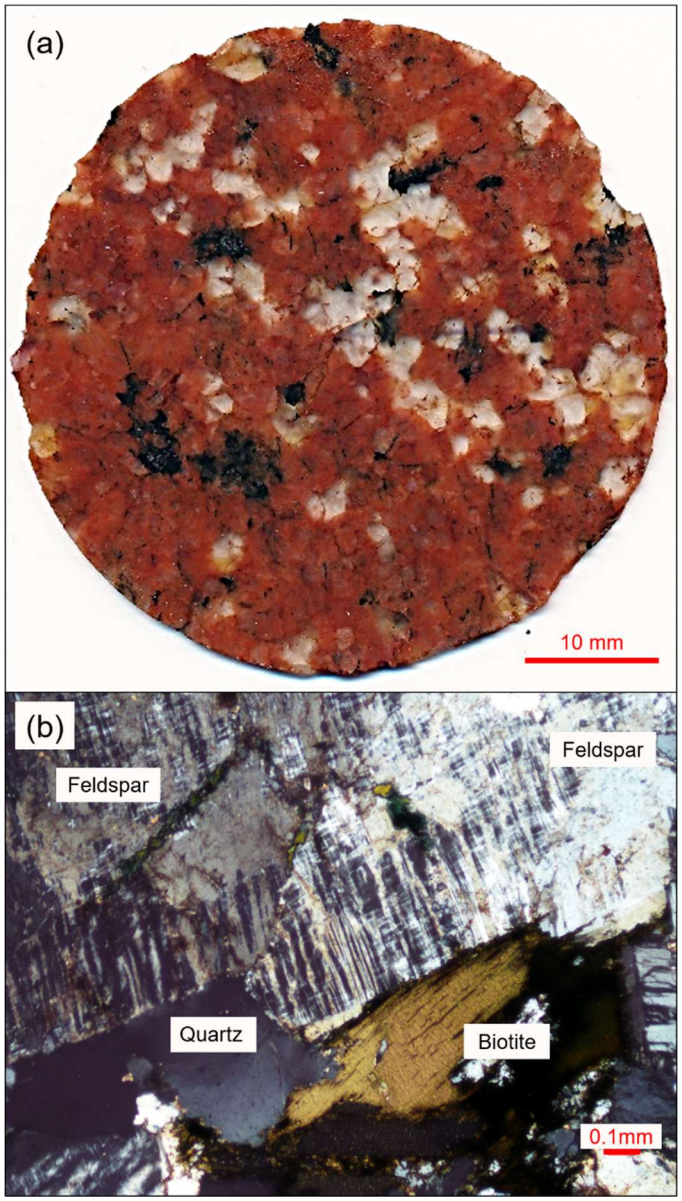

Fig. 1. Wausau granite in (a) disk-shaped specimen, and (b) thin section. The thin section shows feldspar grains with perthitic texture (intergrowth of sodic and potassic feldspar phases).

2.1. *Macro-properties*

The Wausau granite was geomechanically characterized using Uniaxial Compressive Strength (UCS) tests in this study. The UCS tests were executed on cylindrical specimens of approximately 51.4 mm in diameter, with a length-to-diameter ratio of 2.5:1. According to the results of eleven UCS tests, the peak strength ranges from 204 MPa to 260 MPa. Complete stress-strain information was registered in three UCS tests. The Young's modulus (E), Poisson's ratio (ν), crack initiation stress (CI) and crack damage stress (CD) were determined from the strain-stress curves of those three tests. The CD was calculated using the volumetric strain (ε_v) method (Martin and Chandler, 1994), whereas the CI was estimated using the crack volumetric strain ($\varepsilon_{v,c}$) method (Nicksiar and Martin, 2012). Table 1 summarizes the average macro-mechanical properties of Wausau granite based on three UCS tests with complete strain-strain information.

Table 1. Experimental macro-mechanical properties of Wausau granite, expressed in terms of arithmetic mean and two standard deviations (i.e., $\mu \pm 2\sigma$).

Property	Value
Density, ρ_m (kg/m3)	2600 ± 20
Uniaxial Compressive Strength, UCS (MPa)	209 ± 18
Crack initiation threshold, CI (MPa)	91 ± 29 (≈ 44% UCS)
Crack damage threshold, CD (MPa)	196 ± 19 (≈ 94% UCS)
Young's Modulus, E_m (GPa)	69.6 ± 2.8
Poisson's Ratio, ν_m	0.24 ± 0.06

2.2. *Block and Contact Constitutive Models*

In this study, the mineral grains within the BBMs are modeled as unbreakable elastic blocks. Considering that this study is focused on the prediction of the pre-peak macro-mechanical properties (i.e., UCS, CI, CD, Em, νm) of rock specimens, such a simplification is expected to have a negligible effect on the results of the numerical simulations (Sinha and Walton, 2020). Previous studies use a similar simplification criterion for their BBMs (Kazerani and Zhao, 2010; Lan et al., 2010; Chen and Konietzky, 2014; Ghazvinian et al., 2014; Nicksiar and Martin, 2014; Farahmand and Diederichs, 2015; Chen et al., 2016). This simplification helps to save computational time.

The applied block micro-properties correspond to an elastic constitutive model with specific density, Young's modulus, and Poisson's ratio for each mineral type. The grain contacts are modeled following a Coulomb slip-joint constitutive model with residual strength properties. As failure progresses in the simulations, the contacts are assumed to transition their cohesion, friction, and tensile strength to residual values (Nicksiar and Martin, 2014).

2.3. *Micro-properties*

The grain and contact micro-properties applied to the BBMs are taken from the study of Farahmand and Diederichs (2015), who calibrated the micro-properties of Lac du Bonnet granite using BBMs. Given the similarities in mineral composition of Wausau granite and Lac du Bonnet granite (which has an average UCS of 200 MPa; Farahmand and Diederichs, 2015), it is expected that such calibrated parameters in combination with the BBM grain structure used should be able to deliver a reasonable estimation of the strength of Wausau granite. This

assumption supposes that the physics of the models (including the influence of grain structure) are a close approximation of reality.

The mineral composition of Wausau granite was modeled considering a total of four types of grains (K-feldspar, plagioclase, quartz, and biotite) with ten corresponding types of grain-to-grain contacts. The calibrated micro-properties from the study of Farahmand and Diederichs (2015) were directly applied to the models. Tables 2 and 3 summarize the applied grain and contact micro-properties, respectively. As in previous studies, the residual values of tensile strength and cohesion are assumed to be zero (Ghazvinian et al., 2014; Nicksiar and Martin, 2014; Farahmand and Diederichs, 2015).

Table 2. Grain micro-properties (Bass, 1995; Mavko et al., 2003).

Mineral Type	Elastic Modulus (GPa)	Poisson's ratio	Density (g/cc)
K-Feldspar	69.8	0.28	2.56
Plagioclase	73.7	0.26	2.63
Quartz	94.5	0.08	2.65
Biotite	33.8	0.36	3.05

Table 3. Contact micro-properties calibrated by Farahmand and Diederichs (2015).

Contact Type	K_n (GPa/m)	K_s/K_n	C (MPa)	φ, φ_r (°)	σ_t (MPa)
KF / KF	2.3E+5	0.65	110.0	62.0, 5.0	35.0
KF / PL	2.1E+5	0.65	108.0	61.0, 5.0	32.0
KF / QZ	2.7E+5	0.65	76.0	53.0, 5.0	28.2
KF / BT	2.3E+5	0.65	60.0	48.0, 5.0	11.4
PL / PL	2.5E+5	0.65	112.0	63.0, 5.0	37.0
PL / QZ	2.3E+5	0.65	80.0	49.0, 5.0	28.2
PL / BT	2.3E+5	0.65	54.0	45.0, 5.0	22.4
QZ / QZ	2.8E+5	0.65	130.0	65.0, 5.0	35.0
QZ / BT	2.3E+5	0.65	57.0	52.0, 5.0	23.4
BT / BT	1.3E+5	0.65	88.0	55.0, 5.0	25.3

3. GENERATION OF BONDED BLOCK MODELS

The two-dimensional grain structures used in this study were generated as cross-sections from a 3D Voronoi structure developed in Neper, which is an open-source software package for polycrystal generation and meshing in 2D and 3D (Quey, 2019). Neper consists of three modules for generation, meshing, and visualization of tessellations. Neper generates grain assemblies using Voronoi tessellations with convex-shaped cells within spacial domains of different configurations (e.g., prismatic, cylindrical, and circular shapes). Neper allows the definition of cell morphological properties using statistical distributions, specifically cell size (or equivalent diameter) and sphericity, to be employed in the generation of Voronoi tessellations. If the centroids of the cells are known, this aspect can also be defined in Neper as a basis for the tessellations. Neper also offers an option for the generation of two-scale Voronoi tessellations, which involves partitioning every cell of a "primary" Voronoi tessellation into "secondary" Voronoi tessellation cells (Ghazvinian et al., 2014; Wang and Cai, 2018).

Each BBM generated for this study represents a cylindrical core specimen with a diameter of 51.4 mm and a length of 128.5 mm. The mineral grains within the models are represented as convex polygons. Each BBM depicts different grain morphological properties (i.e., grain size, and shape). A 2D baseline Voronoi BBM was defined to represent the average mineral composition, average grain size, equivalent number of grains, and approximate average grain shape of Wausau granite. The mineralogical composition was based on the results of the automated mineralogy analyses. Measurements of the apparent grain size made on disk-shaped specimens of Wausau granite were used to define the average grain size of the baseline model (d = 2.0 mm) and the corresponding equivalent number of grains (39000). According to thin-section microscopy and macroscopic observations, grains tend to show a prismatic shape, rather than uniform rounded shapes like the ones used in previous studies (Chen and Konietzky, 2014; Fabjan et al., 2015; Chen et al., 2016). An average grain shape was defined to represent an intermediate degree of sphericity (s = 0.80) that qualitatively resembles the average shape of a real mineral grain (see Figure 2).

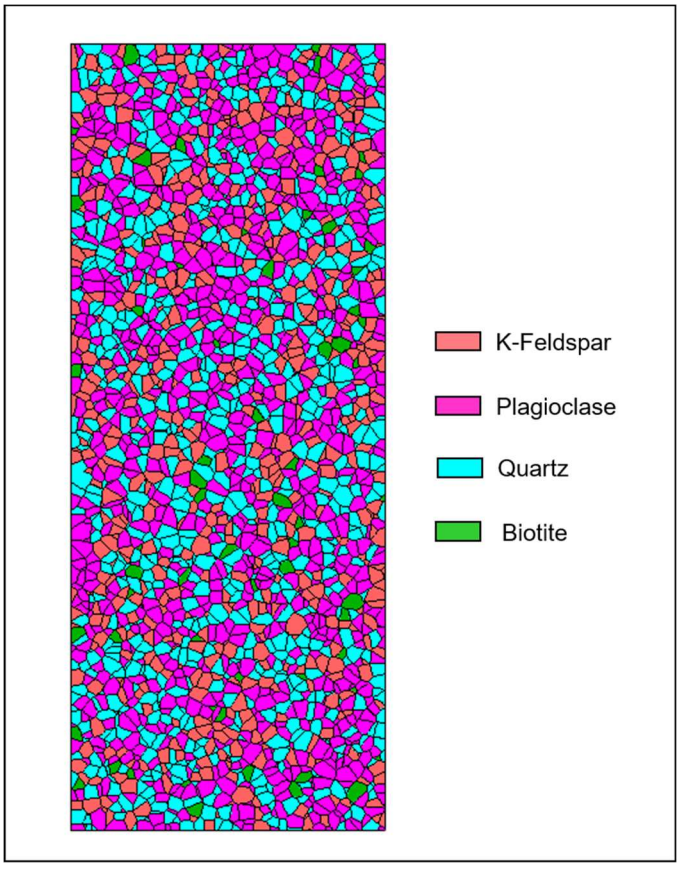

Fig. 2. Two-dimensional Baseline BBM.

Additionally, another six 2D BBMs were constructed. Two of these BBMs were assigned the same characteristics of the baseline model except for grain arrangement. Another two BBMs were based on the same mineral composition, average grain size, and equivalent number of grains as the baseline BBM but were assigned different grain shape (i.e., degree of sphericity). Thus, one model was assigned a low degree of sphericity (s = 0.75), and another was assigned a high degree of sphericity (s = 0.85). Finally, another two BBMs were developed with the same mineral composition and average grain shape as the baseline model but were assigned different average grain sizes: d = 2.3 mm for a model with 27000 grains, and d = 2.8 mm for a model with 15000 grains.

4. NUMERICAL SIMULATION SETUP

The simulations were run in the program UDEC 6.0 (Itasca Consulting, 2014). For the UCS test simulations, axial loading was applied via a constant vertical velocity directly to the top and bottom surfaces of the model (-v/2 and v/2, respectively) to produce an effective loading velocity, v. Given the great influence of the loading velocity on the modeling results, a sensitivity analysis of the loading velocity was performed to determine a proper loading rate that ensures quasi-static equilibrium conditions for the model. A constant velocity of 0.1 m/s was established as a loading velocity below which changes in velocity have limited influence (< 4%) on the model results. For a loading rate of 0.1 m/s, the equivalent rate of 10^{-5} mm/step implies that over 100,000 steps are required to produce a displacement of 1 mm (Lisjak et al., 2014; Gao et al., 2016; Wang and Cai, 2018).

The axial and lateral strains were tracked through multiple pairs of control grid points. In both cases, the strain was calculated by averaging the displacements between the pairs of control points using a FISH script (Itasca, 2014). As shown in Figure 3, five pairs were arranged for tracking the axial strains, and eleven pairs were arranged for tracking the lateral strains. The control grid points were located on the edges of the models. The axial stress was tracked and calculated by averaging the axial stresses (σ_{zz}) measured in the zones of the blocks inside the core specimen through a FISH script. All the zones within the model were considered for this calculation.

5. COMPARATIVE ANALYSIS

The goal of this analysis was to compare the results of laboratory-scale simulations run on BBMs with different representations of the same Wausau granite grain structure and the same set of micro-properties. The comparative analysis focused on the impact of the following parameters: (a) grain arrangement, (b) grain shape, and (c) grain size.

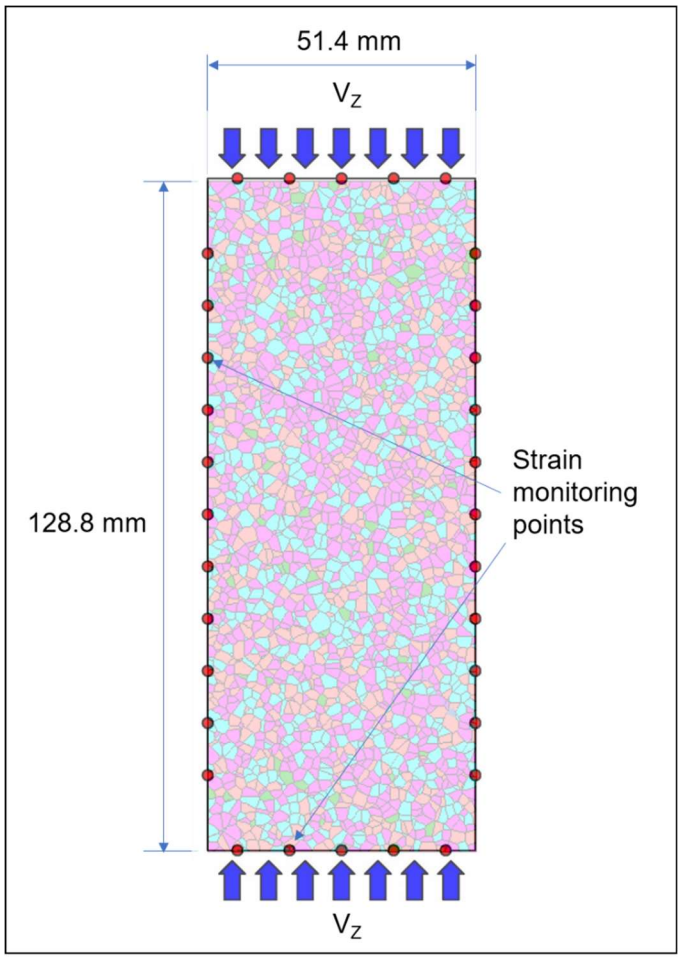

Fig. 3. Configuration for UCS test simulations.

A baseline model was used as a reference for the analysis of the different cases. The baseline BBM represents the average mineral composition and approximate grain geometry of Wausau granite. Figure 4 shows the stress-strain curve obtained from the UCS test simulation using the baseline BBM compared to the average stress-strain curve of the Wausau granite specimens.

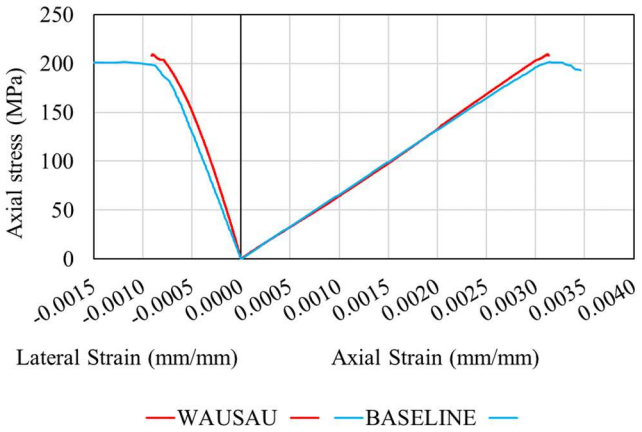

Fig. 4. Stress-strain curves for the average UCS experimental results of Wausau granite and baseline UCS test simulation.

The baseline simulation provides a reasonable approximation of the of the Wausau granite response to loading. Note that because of the brittle nature of the Wausau granite, the post-peak behavior was not recorded during the UCS tests, since the specimens under loading failed violently right after they reached the peak strength.

The UCS test simulations were also found to approximate the fracture patterns observed in the laboratory (see Figure 5). The failed laboratory specimens show dominant tensile fractures, but also some minor shear fractures and areas of crushed grains. The simulations show relatively short tensile fractures and macroscopic shear fractures that exist as the coalescence of various smaller tensile and shear fractures.

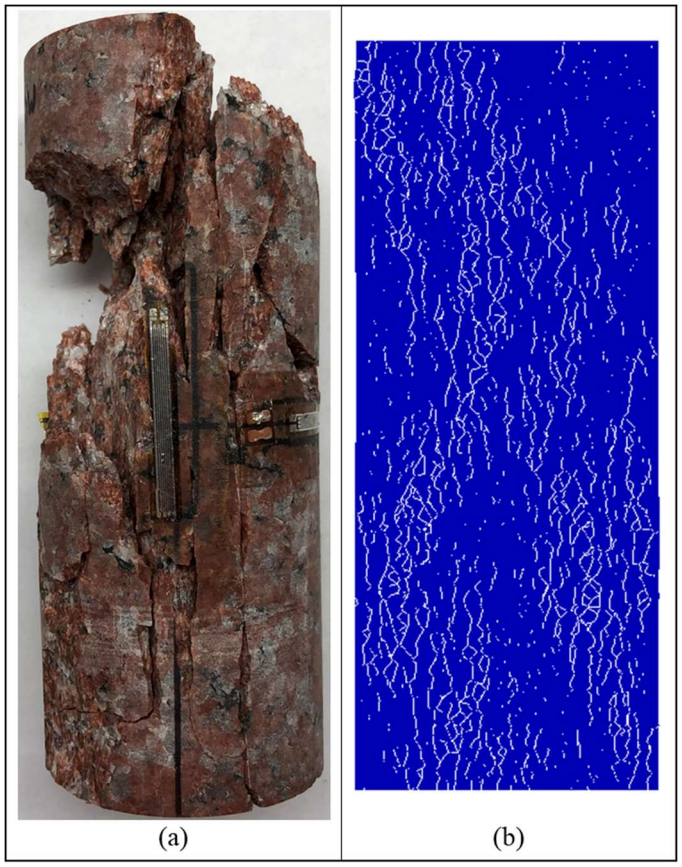

Fig. 5. Failure pattern obtained in a laboratory UCS test (a), and fracture pattern obtained from the baseline UCS test simulation (b).

5.1. Effect of grain arrangement

In order to simulate the influence of grain arrangement variations, three different grain distributions (i.e., positions of individual minerals) were randomly assigned to the same baseline Voronoi grain structure, while maintaining Wausau granite's mineral composition. Thus, the baseline BBM was established as the first case of the analysis ("A"), whereas the other two cases are duplicates of the baseline grain structure but with different grain arrangements ("B" and "C").

Figures 6 to 8 present comparisons of the predicted UCS, CD stress, and CI stress obtained with each of the three different grain distributions in 2D simulations. Each graph shows the predicted macro-property compared to the mean (μ) and 95% confidence interval (μ ± 2σ) of the actual Wausau granite (WAU) properties obtained in laboratory tests. Grain arrangements "A" (baseline, "BL"), "B," and "C" show different results, with differences up to 17% (UCS = 5%, CD = 11%, CI = 17%). The Young's modulus and the Poisson's ratio are apparently not very sensitive to variations in grain arrangement and show differences below 3%.

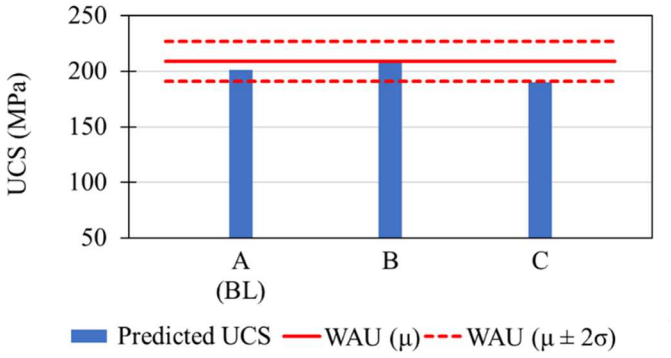

Fig. 6. Comparison of predicted UCS using BBMs with different grain arrangement.

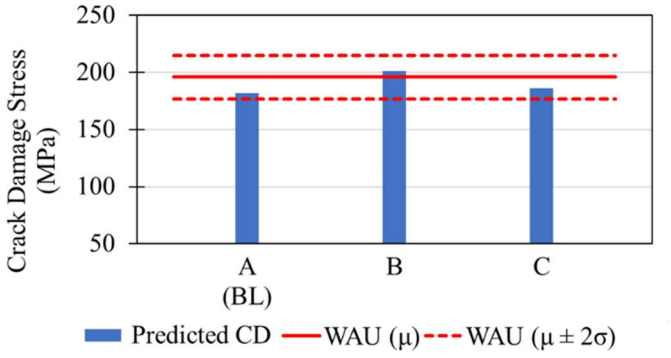

Fig. 7. Comparison of predicted CD stress using BBMs with different grain arrangement.

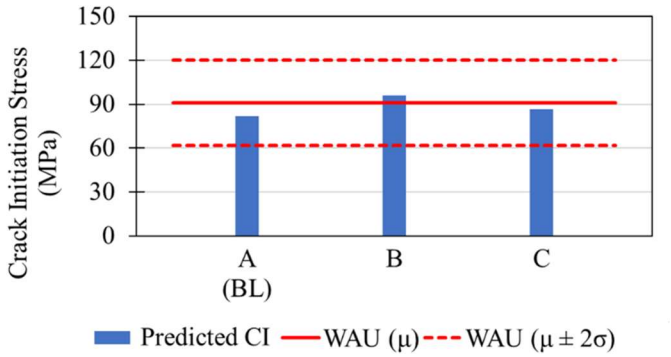

Fig. 8. Comparison of predicted CI stress using BBMs with different grain arrangement.

5.2. *Effect of grain shape*

BBMs with the same mineral composition and number of grains as the baseline block model but different grain shapes were used for this part of the study. The grain shape was expressed as a function of sphericity in Neper (Quey, 2019) and represented in three different BBMs. The sphericity was defined as the ratio between the surface area of the sphere of equivalent volume and the surface area of the polyhedral grain. Sphericity has a maximum value of 1 for a spherical grain (Quey and Renversade, 2018; Quey, 2019).

The first model depicts grains with high sphericity (i.e., sphericity = 0.85) similar to the rounded shape typically employed in BBMs. The second model represents grains with an intermediate degree of sphericity (i.e., sphericity = 0.80) that resembles the average shape of actual mineral grains within Wausau granite; this intermediate degree of sphericity is as used in the baseline BBM. The third model denotes an assembly of grains with low sphericity (i.e., sphericity = 0.75), characterized by exaggerated angularity and slightly elongated shapes.

The results of the simulations do not show a clear correlation between the predicted UCS values and the degree of sphericity represented in some of the models (see Figure 9). However, the representation of grains with low sphericity predicted a significantly higher value of UCS, compared to the baseline model results. This effect can be explained by the degree of interlocking among grains, which increases when the grains are more irregular (i.e., low sphericity), and directly influences the peak strength of the rock.

The predictions of CD stress, CI stress (see Figures 10 and 11) do not show any apparent direct correlation with the variations of grain shape but present differences up to 14% (CD = 14%, CI = 4%). The elastic parameters (i.e., Young's modulus and Poisson's ratio) show differences below 2% and are not very sensitive to grain shape variations.

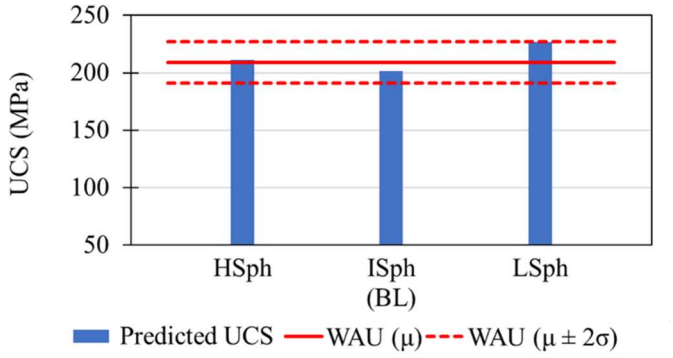

Fig. 9. Comparison of predicted UCS using BBMs with different grain shape.

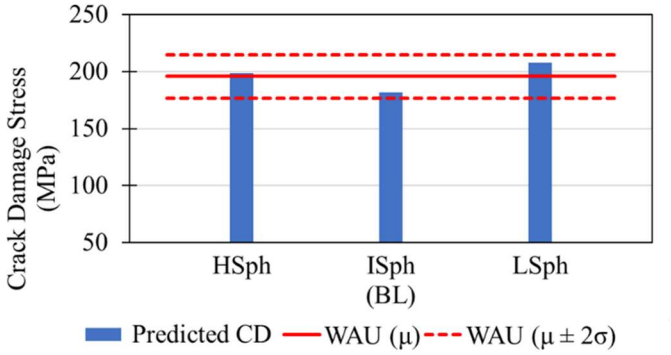

Fig. 10. Comparison of predicted CD stress using BBMs with different grain shape.

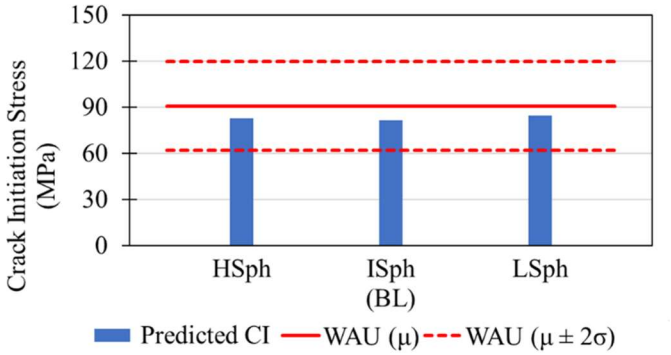

Fig. 11. Comparison of predicted CI stress using BBMs with different grain shape.

5.3. *Effect of grain size*

This part of the study used three BBMs with different average grain size, but the same mineral composition. The first BBM (baseline model) represents an average grain diameter of 2.0 mm, whereas the second and third models have average equivalent diameters of 2.3 mm and 2.8 mm, respectively.

The results obtained in this analysis do not show a clear influence of the grain size on the prediction of macro-properties. However, a rough correlation was detected in Young's modulus prediction, where an increase of the grain size appears to lead to a slight increase in the value of elastic modulus (see Figure 12). Such an increase in elastic modulus is probably related to elastic behavior assigned to the grains within the BBMs. Larger elastic grains add stiffness to the whole system, as the number of softer grain-boundary elements is decreased. Figures 13 to 15 show the results of this analysis for UCS, CD stress, and CI stress, which reach differences up to 13% (UCS = 10, CD = 4%, CI = 13%). Similar to previous analyses, the Poisson's ratio does not exhibit significant sensitivity to grain size changes and presents differences below 2%

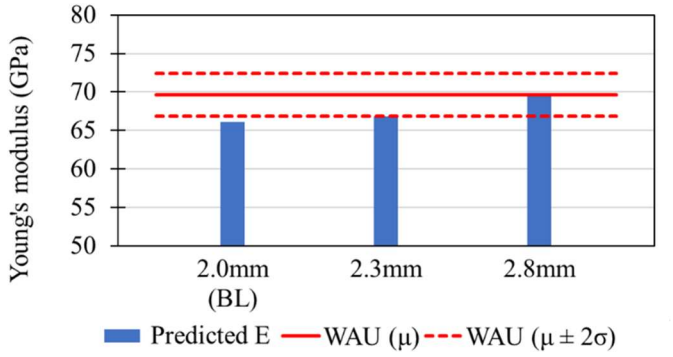

Fig. 12. Comparison of predicted Young's modulus using BBMs with different grain size.

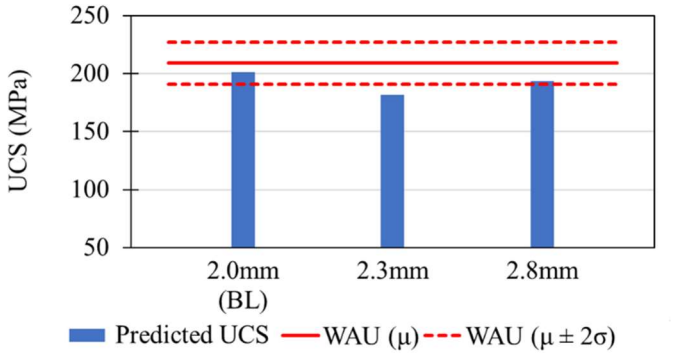

Fig. 13. Comparison of predicted UCS using BBMs with different grain size.

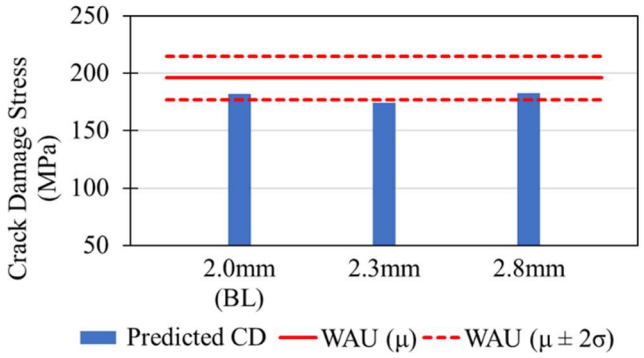

Fig. 14. Comparison of predicted CD stress using BBMs with different grain size.

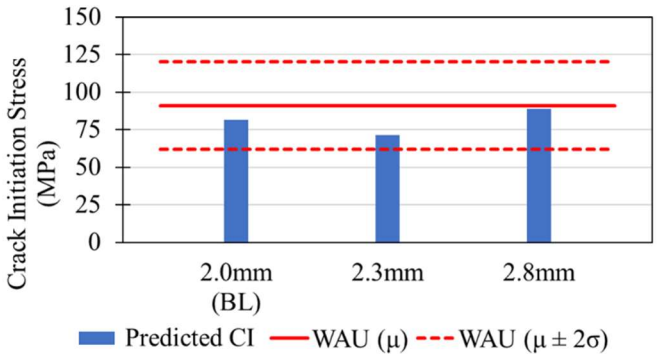

Fig. 15. Comparison of predicted CI stress using BBMs with different grain size.

6. DISCUSSION AND CONCLUSIONS

The results of the simulations in this study show that slight changes in the representation of certain geometric parameters of the grain structure can have an impact on the prediction of rock mechanical behavior. Table 4 summarizes the degree of influence of the representation of different factors expressed in terms of predicted UCS, compared to the values obtained using the baseline BBM in combination with micro-properties from Farahmand and Diederichs (2015). Figure 16 shows the stress-strain curves for all the compared cases.

Grain arrangement variations had a minor influence on the results of the simulations, producing about 5% variation in the predicted UCS. Although grain arrangement heterogeneity is an expected issue when dealing with geo-materials such as rocks and its effect cannot be prevented, it is necessary to control and minimize its uncertainty in numerical models to predict the rock's mechanical behavior with reasonable accuracy. Alternatively, multiple models with different grain arrangement realizations can be conducted to assess a range of possible behaviors.

Grain shape variations presented a significant influence on the results of the simulations, particularly affecting the degree of interlocking among grains and, consequently, the simulated peak strength. Such an effect is noticeable when the grains have lower than typical sphericity, resulting in a UCS value 13% higher than the baseline corresponding to a slightly lower sphericity value. Considering the UCS variability of actual specimens of Wausau granite (see Table 1), the predictions made using BBMs with inadequate representations of grain shape (i.e., low sphericity) can be considered of low accuracy.

Table 4. Influence of different representations on the predicted UCS.

CASE	UCS (MPa)	Difference (%)
BASELINE (arrangement "A", sphericity = 0.80, diameter = 2.0 mm)	201	N/A
AR-B (arrangement "B")	210	4.2
AR-C (arrangement "C")	190	-5.4
S-0.75 (sphericity = 0.75)	226	12.6
S-0.85 (sphericity = 0.85)	211	4.9
D-2.3 (diameter = 2.3 mm)	182	-9.6
D-2.8 (diameter = 2.8 mm)	193	-3.9

The simulations show noticeable influence of the grain size representation in the model's predicted UCS (up to 10%). However, such an effect is likely to be related to the associated grain arrangement variability induced by the grain size variations based on the lack of a coherent trend in the UCS as a function of average grain size.

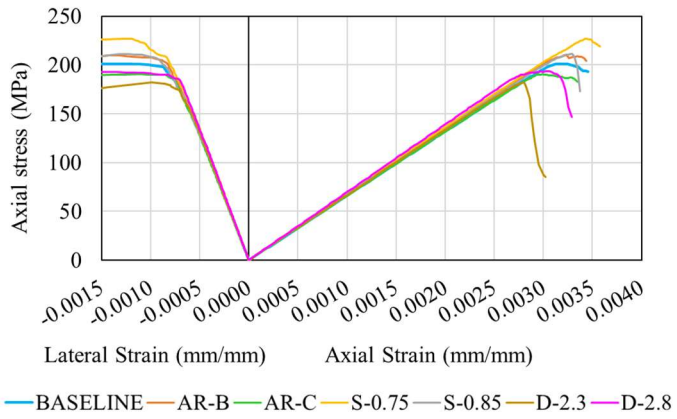

Fig. 16. Stress-strain curves for the seven compared cases.

The results of this study show that a BBM that properly represents the grain structure of a rock (i.e., grain size, grain shape, and relative mineral proportions) can be used in combination with previously published calibrated micro-properties to predict rock strength, as was done with the Wausau granite. The effects of grain size and grain shape can be approximated to provide a reasonable representation of the grain structure using a Voronoi approach. Such a grain structure can then be used for the prediction of rock strength in combination with properly calibrated micro-properties.

There is a complex interaction between approximations made in the Voronoi BBM grain structure used for micro-property calibration and the resulting influences on the micro-properties. If a set of micro-properties was derived using an inappropriate grain structure, they will likely not be useful for predictive modeling. Alternatively, it may not be possible to predict the laboratory-scale stress-strain behavior of a given rock using previously determined micro-properties if the rock in question has a grain structure that deviates significantly from what can be approximated using a Voronoi representation.

ACKNOWLEDGEMENTS

The authors wish to express their acknowledgements to the National Institute for Occupational Safety and Health (NIOSH) for providing financial support to conduct this study.

REFERENCES

1. Chen, W., and H. Konietzky. 2014. Simulation of heterogeneity, creep, damage and lifetime for loaded brittle rocks. *Tectonophysics*, 633(1), 164–175.

2. Chen, W., H. Konietzky, X. Tan, and T. Frühwirt. 2016. Pre-failure damage analysis for brittle rocks under triaxial compression. *Computers and Geotechnics*, 74, 45–55.

3. Fabjan, T., D.M. Ivars, and V. Vukadin. 2015. Numerical simulation of intact rock behavior via the continuum and Voronoi tessellation models: A sensitivity analysis. *Acta Geotechnica Slovenica*, 12(2), 5–23.

4. Farahmand, K., and M.S. Diederichs. 2015. A calibrated synthetic rock mass (SRM) model for simulating crack growth in granitic rock considering grain-scale heterogeneity of polycrystalline rock. In *Proceedings of the 49th US Rock Mechanics/Geomechanics Symposium*, San Francisco, California.

5. Gao, F., D. Stead, and D. Elmo. 2016. Numerical simulation of microstructure of brittle rock using a grain-breakable distinct element grain-based model. *Computers and Geotechnics*, 78, 203–217.

6. Ghazvinian, E., M.S. Diederichs, and R. Quey. 2014. 3D random Voronoi grain-based models for simulation of brittle rock damage and fabric-guided micro-fracturing. *Journal of Rock Mechanics and Geotechnical Engineering*, 6(6), 506–521.

7. Itasca Consulting Group Inc. 2014. UDEC version 6.0: Universal distinct element code, user's guide (4th ed.).

8. Jing, L. 2003. A review of techniques, advances and outstanding issues in numerical modelling for rock mechanics and rock engineering. *International Journal of Rock Mechanics and Mining Sciences*, 40, 283–353.

9. Jing, L., and J.A. Hudson. 2002. Numerical methods in rock mechanics. *International Journal of Rock Mechanics and Mining Sciences*, 39, 409–427.

10. Kazerani, T., and J. Zhao. 2010. Micromechanical parameters in bonded particle method for modeling of brittle material failure. *International Journal for Numerical and Analytical Methods in Geomechanics*, 34(January 2010), 1877–1895.

11. LaBerge, G.L., and P.E. Myers. 1983. Precambrian Geology of Marathon County, Wisconsin. Wisconsin Geological and Natural History Survey, Information Circular 45, 88.

12. Lan, H., C.D. Martin, and B. Hu. 2010. Effect of heterogeneity of brittle rock on micromechanical extensile behavior during compression loading. *Journal of Geophysical Research*, 115(B01202).

13. Lisjak, A., and G. Grasselli. 2014. A review of discrete modeling techniques for fracturing processes in discontinuous rock masses. *Journal of Rock Mechanics and Geotechnical Engineering*, 6(4), 301–314.

14. Liu, G., M. Cai, and M. Huang. 2018. Mechanical properties of brittle rock governed by micro-geometric heterogeneity. *Computers and Geotechnics*, 104(January), 358–372.

15. Martin, C.D., and N.A. Chandler. 1994. The progressive fracture of Lac du Bonnet granite. *International Journal of Rock Mechanics and Mining Sciences*, 31(6), 643–659.

16. Nicksiar, M., and C.D. Martin. 2012. Evaluation of methods for determining crack initiation in compression tests on low-porosity rocks. *Rock Mechanics and Rock Engineering*, 45(4), 607–617.

17. Nicksiar, M., and C.D. Martin. 2014. Factors affecting crack initiation in low porosity crystalline rocks. *Rock Mechanics and Rock Engineering*, 47(4), 1165–1181.

18. Potyondy, D.O., and P.A. Cundall. 2004. A bonded-particle model for rock. *International Journal of Rock Mechanics and Mining Sciences*, 41(8 SPEC.ISS.), 1329–1364.

19. Quey, R. 2019. Neper reference manual. *Retrieved from http://neper.sourceforge.net/index.html*

20. Quey, R., and L. Renversade. 2018. Optimal polyhedral description of 3D polycrystals: Method and application to statistical and synchrotron X-ray diffraction data. *Computer Methods in Applied Mechanics and Engineering*, 330, 308–333.

21. Sims, P.K., K.J. Schulz, E. Dewitt, and B. Brasaemle. 1993. Petrography and Geochemistry of Early Proterozoic Granitoid Rocks in Wisconsin Magmatic Terranes of Penokean Orogen, Northern Wisconsin. U.S. *Geological Survey Bulletin* 1904-J, 1–31.

22. Sinha, S., and G. Walton. 2020. A study on Bonded Block Model (BBM) complexity for simulation of laboratory-scale stress-strain behavior in granitic rocks. *Computers and Geotechnics*, 118, 103363.

23. Wang, X., and M. Cai. 2018. Modeling of brittle rock failure considering inter- and intra-grain contact failures. *Computers and Geotechnics*, 101(April), 224–244.